Effect of flexural stress on fabrication and optical properties of a composite photonic material

Devon Courtwright, Sangeeta Rout, Jakeem Adrien, Mikhail A. Noginov
Norfolk State University, Faculty Group, Center for Materials Research, 700 Park Avenue, Norfolk, USA, 23504

Abstract. We spin coated thin films of PMMA polymer doped with HITC laser dye onto microscope cover slides under applied flexural stress and found the patterns of scattering (milkiness) to correlate with the spatial variation of the pressure pattern. We further deposited thin gold films on top of the HITC:PMMA films and measured highly unusual transmission spectra of Au collected from strongly deformed (stressed) local areas of the sample. These spectra, which strongly deferred from those of plain Au films deposited onto unstressed glass, could not be described by simple, e.g. Maxwell Garnett, effective media models, calling for a thorough theoretical study.

Keywords: photonic metamaterials, composite optical materials, effective medium approximation, flexural stress.

E-mail: mnoginov@nsu.edu

The last two decades have witnessed rapid growth of photonic metamaterials – engineered composite materials, comprised of rationally designed nanoscopic (often metallic) inclusions embedded into a dielectric matrix [1-3]. Theoretically predicted and experimentally demonstrated applications and functionalities of metamaterials and related nanophotonic structures include negative index of refraction [4,5], invisibility optical cloaking [6,7], nanocircuits operating at optical frequencies [8], optical topological insulators [9,10], artificial intelligence [11], and many others. Historically, most metamaterials have been fabricated in cleanroom environments (using a "top-down" engineering approach) and their sizes did not exceed ~100 μm x 100 μm [1-3]. At the same time, real-life applications (including photovoltaics [12], thermal radiation control [13], and multi-functional conformal coatings [14]) call for inexpensive "bottom-up" mass-produced metamaterials [15-18], whose dimensions exceed a square inch (or a square meter) and whose responses to electromagnetic waves can be tuned at the fabrication stage or in situ. The latter demand motivated the present study of the

polymer-gold composite material, whose optical properties can be easily controlled by a flexural stress applied to a thin glass substrate.

In sample preparation, poly(methyl) methacrylate (PMMA) polymer (with an average molecular weight 120,000) was dissolved in a dichloromethane (DCM) solvent, in concentration 116 g/l, and sonicated, at room temperature, for a total of 90 minutes. A laser dye, 2-[7-(1,3-Dihydro-1,3,3-trimethyl-2H-indol-2-ylidene)-1,3,5-heptatrienyl]-1,3,3-trimethyl-3H-indolium iodide (HITC), was added to the polymer solution for better visibility, as discussed below, in the concentration 30 g/l (in solid state). The solution was then spin coated onto 0.2 mm thick glass cover slips from VWR, using a 6800 Spin Coater from Specialty Coating Systems with an applied vacuum pressure of approximately 2 psi (according to the manufacturer's specifications). The spin coating was performed at 555 RPM for 3 seconds, followed by 5000 RPM for 25 seconds, and finally at 7500 RPM for 16 seconds. By using the relatively high concentration of PMMA in DCM, the films were intentionally made scattering (milky) to provide for visibility of the patterns discussed below, Fig. 1a.

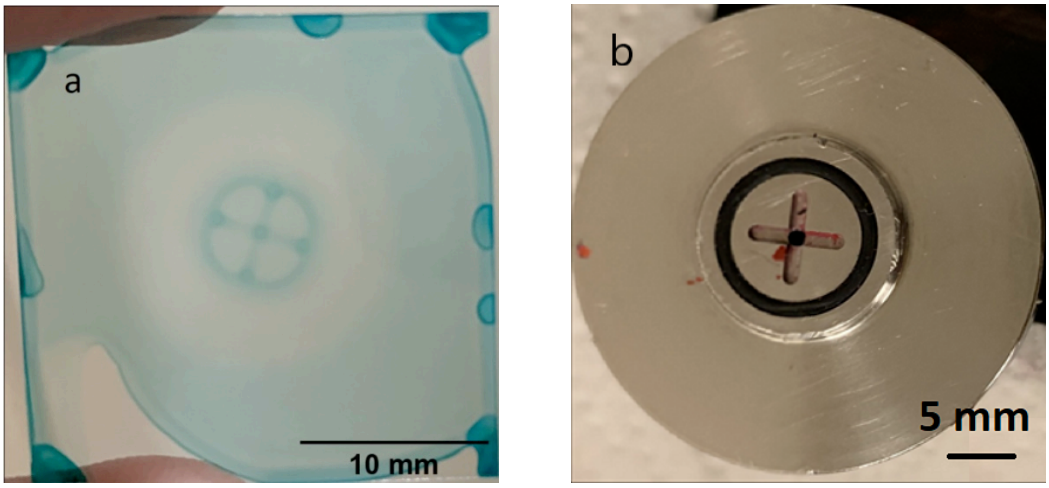

Figure 1: (a) HITC:PMMA film deposited onto 25x25 mm glass slip at applied flexural stress (vacuum suction). (b) Photograph of the chuck holding the sample, showing the hole for the vacuum suction, two slits forming a cross, elevated metallic ring and the rubber o-ring (black).

The chuck of the spin coater, holding the sample by applied vacuum, had a small hole in the center for a vacuum suction, o-ring for keeping the vacuum, and two slits (forming a cross) for a uniform distribution of the vacuum, Fig. 1b. As we see below, the latter functionality was not highly efficient and the stress applied to the sample by vacuum (strictly speaking, by atmospheric pressure) was highly non-uniform. As the vacuum was turned on, the glass slip bent, forming a bowl shape. Subsequently, the PMMA film was deposited onto a curved surface. In the end of the spinning cycle, when the rotation stopped, the vacuum was broken and the glass substrate with the deposited HITC:PMMA film popped up, becoming plane again.

Almost instantaneously, an intense greenish-bluish image of the cross and the ring appeared and become clearly visible (the greenish-bluish coloration was characteristic of HITC dye and was never observed in PMMA films without dye), Fig. 1a. This observation, suggesting that the flexural stress provided by vacuum is strongly inhomogeneous at the 1 mm scale, is one of the most intriguing results of this study. The thickness of the HITC:PMMA film measured (using DekTak XT stylus profilometer from Bruker) in the arm of the cross, 120 nm ±10%, was similar, within the experimental error, to that measured outside or the cross. We infer that the intense coloration of the cross and the ring were due to smaller amount of scattering in the respective local areas, determined by local non-uniformity of the flexure stress. (An alternative explanation accounting for a segregation of the dye molecules and their higher concentrations in the positions of the cross and the ring appears to be less likely.)

We then deposited thin Au films (using a Nano 36 thermal evaporator from Kurt J. Lesker) on top of HITC:PMMA films, with the images of the cross and the ring described above (Fig. 1a), photographed them (Fig. 2), and took their transmission and reflection spectra (using a Lambda 900 spectrophotometer, PerkinElmer) from the local areas corresponding to the arms of the cross and the spots outside of the ring and the cross (Fig. 3). The size of the light spot on the sample was 3.6 mm x 1.3 mm in the transmission experiments and 8 mm x 1.2 mm in the reflection experiments.

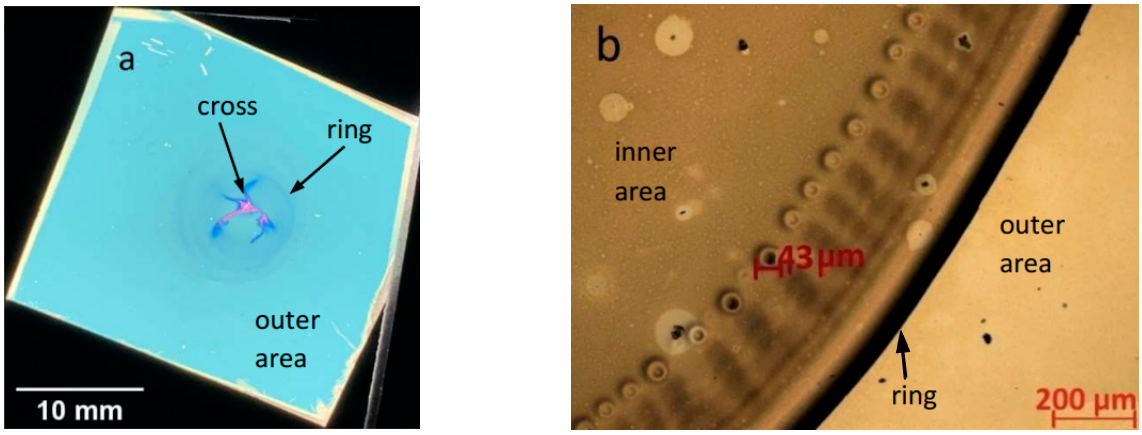

Figure 2: (a) Photograph of the glass slip sample with deposited HITC:PMMA and Au films, taken in the transmission mode. The greenish-bluish coloration dominating the area of the sample is characteristic of "regular" unstressed Au films, the deformed cross is pink and blue, while the ring surrounding the cross is grayish-bluish. (b) Photograph of the ring taken in the reflection mode. The 43 µm "crater" is one of many "open sphere" features created in the ring area in the course of fabrication.

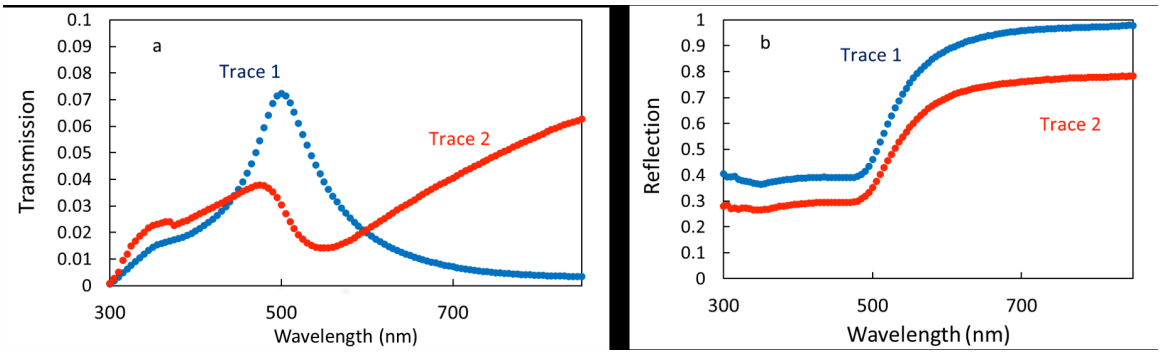

Figure 3: Transmission (a) and reflection (b) spectra of the HITC:PMMA films measured outside of the ring (trace 1) and in the position of the cross' arm (trace 2).

Outside of the cross and the ring, the transmitted light was greenish-bluish (Fig. 2a), characteristic of thin Au films [19,20], and the transmission spectrum featured the well known peak at 500 nm, trace 1 in Fig. 3a. By comparing the experimental transmission spectrum with the one calculated using the on-line transfer matrix solver [21], we evaluated the thickness of the gold film to be equal to 61 nm, while the thickness determined using the profilometer was ~40 nm. The characteristic reflection spectra of the "outer" area (outside of the ring) were typical of thin Au films, trace 1 in Fig. 3b.

At the same time, the transmission of the local areas with the patterned cross was strikingly different from that described above. Thus, in the arms of the cross, the transmitted light was pink and dark blue, see Fig. 2a. The corresponding transmission spectrum had the maximum at $\lambda \approx 470$ nm, the minimum at $\lambda \approx 550$ nm, and the growth (with increase of the wavelength) at $\lambda \geq 550$ nm, trace 2 in Fig. 3a. (In this particular measurement, the size of the focused light spot, 3.6 mm x 1.3 mm, was commeasurable with the arm of the cross, ~3 mm x 1 mm.) The corresponding reflection spectrum was not much different from that measured outside of the cross and the ring (Fig. 3b, trace 2), possibly because the size of the light spot in the

reflection measurements (~8 mm x 1.2 mm) was significantly larger than the size of the cross' arm and most of the reflected light was coming from the low-stressed area. Microphotographs of the gold-coated samples showed neat rows of ~10 μm cavities or craters, Fig. 2b. However, the morphology features determining the color and the spectra of the transmitted light must be much smaller.

The dip in transmission at $\lambda \approx 550$ nm followed by the transmission's growth at the longer wavelengths is characteristic of gold nanospheres embedded into a dielectric matrix [22]. Therefore, we attempted to fit the transmission and reflection spectra of the HITC:PMMA:Au films using the Maxwell Garnett model [23] (for Au nanospheres in the HITC:PMMA matrix). Toward this end, the effective medium spectra of the composite materials were calculated using the formula:

$$\epsilon_{eff} = \frac{2f\epsilon_h(\epsilon_i - \epsilon_h) + \epsilon_h(\epsilon_i + 2\epsilon_h)}{(\epsilon_i + 2\epsilon_h) - f(\epsilon_i - \epsilon_h)} \quad (1)$$

where f is the filling fraction of inclusions, ϵ_h is the permittivity of the host material (HITC:PMMA), ϵ_i is the permittivity of the inclusions (Au) and ε_{eff} is the permittivity of effective medium. The spectra of dielectric permittivities of Au and PMMA were taken from Refs. [24,25] and [26], respectively.

We further used the analytical formulas derived in Ref. [27] to calculate the reflection and transmission spectra of a three-layered structure, such as glass/HITC:PMMA:Au/air (assuming the thickness of the Au film to be 61 nm). Although a qualitative (but not quantitative) agreement between the experimental transmission spectra of the cross and those calculated at Au filling factors $f \leq 0.3$ can be seen (in e.g. Fig. 4a), even a qualitative agreement ceases to exist, for the same filling factors, if the experimental and the calculated reflection spectra are compared to

each other, Fig. 4a. On the other hand, a modest agreement between the experimental and the calculated transmission spectra of the composite material can be found at Au filling factor $f \geq 0.8$, far beyond the range of applicability of the Maxwell Garnett model, when the experimental and the calculated transmission spectra have nothing in common. Note that the disagreement between the theory and the experiment can be partly due to a higher optical loss in our experimental Au films than that reported in the literature [24,25].

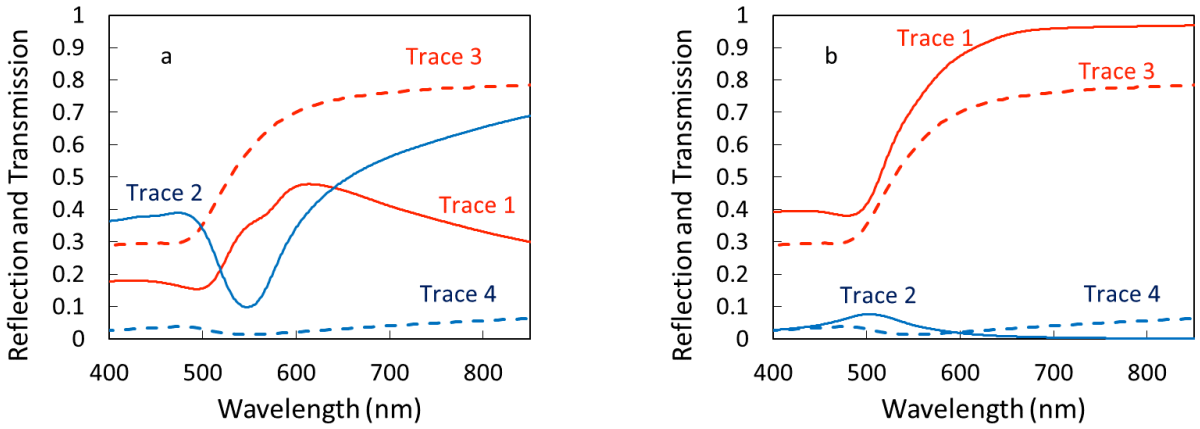

Figure 4: Calculated (traces 1 and 2) and experimental (traces 3 and 4) reflection (traces 1 and 3) and transmission (traces 2 and 4) spectra of the composite HITC:PMMA:Au media, as explained in the text. Au filling factor f=0.2 (a) and f=0.9 (b).

We, thus, conclude that the transmission and the reflection spectra of HITC:PMMA:Au composites cannot be described in term of the Maxwell Garnett model. We further ran the calculations for an "inverted" Maxwell Garnett model (for HITC:PMMA "bubbles" in a gold matrix) and the agreement between the experiment and the calculation was not any better. Application of more complicated effective media theories, such as Bruggeman model [28], Bergman-Milton model [29,30], *etc.*, is the subject of a separate study to be published elsewhere.

To summarize, we have demonstrated that optical properties of HITC:PMMA:Au composite materials can be strongly altered by flexural stress applied to thin glass substrates during the spin coating. (This result is in accord with Ref. [31] reporting on mechanical tuning of optical properties of a metamaterial.) While the pattern of the stress distribution was seen in scattering of HITC:PMMA films without any metal, the gold film, deposited on top of the stressed polymeric film, changed the color of the transmitted light from greenish-bluish to pink or dark blue. Particularly intriguing and important result of this study is the high spatial resolution of the stress pattern determining the composite's optical properties and dispersion, which can find application in controlling incident light and spontaneous emission.

The morphology of the composite material, the spectrum of its effective dielectric permittivity as well as in situ control of the material's optical properties are subjects of further studies to be published elsewhere.

Acknowledgments

U.S. Department of Defense (W911NF1810472); Air Force Office of Scientific Research (FA9550-18-1-0417); National Science Foundation (1830886, 1856515).

References

1. Engheta, N. & Ziolkowski, R. W., (Eds.), Metamaterials: physics and engineering explorations. John Wiley & Sons, (2006).

2. M. A. Noginov, V. A. Podolskiy, Eds. Tutorials in Metamaterials (Series in Nano-optics and Nanophotonics); CRC Press, Taylor & Francis Group: Boca Raton, FL (2011).

3. W. Cai, V. M. Shalaev, Optical Metamaterials: Fundamentals and Applications; Springer (2010).

4. Pendry, J. B., “Negative refraction makes a perfect lens,” Physical review letters, 85(18), 3966, (2000).

5. R. A. Shelby, D. R. Smith, and S. Schultz, “Experimental verification of a negative index of refraction,” Science, 292(5514), 77-79, (2001).

6. D. Schurig, et al, “Metamaterial electromagnetic cloak at microwave frequencies,” Science, 314(5801), 977-980, (2006).

7. W. Cai, et al. “Optical cloaking with metamaterials,” Nature photonics, 1(4), 224-227, (2007).

8. Engheta, N., “Circuits with light at nanoscales: optical nanocircuits inspired by metamaterials,” Science, 317(5845), 1698-1702, (2007).

9. Khanikaev, A. B., et al, “Photonic topological insulators,” Nature materials, 12(3), 233-239, (2013). https://doi.org/10.1038/nmat3520

10. Lu, L., Joannopoulos, J. & M. Soljačić, “Topological photonics,” Nature Photonics 8, 821–829 (2014). https://doi.org/10.1038/nphoton.2014.248

11. Shen, Y., et al. “Deep learning with coherent nanophotonic circuits,” Nature Photonics, 11, 441 (2017).

12. Y. Cui, K. Fung, N. X. Fang, et al. “Ultrabroadband light absorption by a sawtooth anisotropic metamaterial slab,” Nano letters, 12(3), 1443-1447 (2012).

13. Li, W., & Fan, S. “Nanophotonic control of thermal radiation for energy applications,” Optics Express, 26(12), 15995-16021 (2018).

14. Jiang, Z. H., Yun, S., Toor, F., Werner, D. H., & Mayer, T. S. “Conformal dual-band near-perfectly absorbing mid-infrared metamaterial coating,” ACS Nano, 5(6), 4641-4647 (2011).

15. D. Chanda, et al., “Large-area flexible 3D optical negative index metamaterial formed by nanotransfer printing,” Nature Nanotech 6, 402–407 (2011). https://doi.org/10.1038/nnano.2011.82

16. Soukoulis, C. & Wegener, M., “Past achievements and future challenges in the development of three-dimensional photonic metamaterials,” Nature Photonics 5, 523–530 (2011). https://doi.org/10.1038/nphoton.2011.154

17. Mayy, M., et al., “Development of composite silver-polymer metamaterials,” Journal of Applied Physics, 105(8), 084318 (2009).

18. Asane, J. K., et al., “Optical properties of nanoporous gold foams,” AIP Advances, 8(9), 095302 (2018). DOI:10.1063/1.5030128

19. Axelevitch, A., Gorenstein, B. & Golan, G., “Investigation of optical transmission in thin metal films”, Physics Procedia, 32, 1-13 (2012).

20. Rout, S., et al., “Nanoporous gold nanoleaf as tunable metamaterial,” Scientific Reports, 11(1), 1-9 (2021).

21. Ishii, S., et al. (2014), "PhotonicsRT: Wave Propagation in Multilayer Structures," https://nanohub.org/resources/photonicsrt (DOI: 10.4231/D3MK6588C), 27 May 2014.

22. Doremus, R. H., “Optical properties of small gold particles,” The Journal of Chemical Physics, 40(8), 2389-2396 (1964).

23. Markel, V. A., “Introduction to the Maxwell Garnett approximation: tutorial,” JOSA A, 33(7), 1244-1256 (2016).

24. Ni, X., Liu, Z., Kildishev, A. V., "PhotonicsDB: Optical Constants," (2018). https://nanohub.org/resources/photonicsdb. (DOI: 10.4231/D3D795D1M). 30 March 2018

25. Johnson, P. B. & Christy, R. W., “Optical constants of the noble metals,” Physical review B, 6(12), 4370, (1972).

26. Polyanskiy, M. N., “Refractive index database,” https://refractiveindex.info (Accessed 20 August 2020)

27. Raether, H., Surface plasmons on smooth surfaces. In Surface plasmons on smooth and rough surfaces and on gratings (pp. 4-39). Springer, Berlin, Heidelberg (1988).

28. Bruggeman, V. D. “Berechnung verschiedener physikalischer Konstanten von heterogenen Substanzen. I. Dielektrizitätskonstanten und Leitfähigkeiten der Mischkörper aus isotropen Substanzen,” Annalen der Physik, 416(7), 636-664 (1935).

29. Bergman, D. J. "Exactly solvable microscopic geometries and rigorous bounds for the complex dielectric constant of a two-component composite material," Physical Review Letters, 44(19), 1285 (1980).

30. Milton, G. W. "Bounds on the complex permittivity of a two□component composite material," Journal of Applied Physics, 52(8), 5286-5293 (1981).

31. Pryce, I. M., Aydin, K., Kelaita, Y. A., Briggs, R. M. & H. A. Atwater, "Highly Strained Compliant Optical Metamaterials with Large Frequency Tunability," Nano Letters 10(10), 4222-4227, (2010). DOI: 10.1021/nl102684x